Ink-jet printing versus solvent casting to prepare oral films: effect on mechanical properties and physical stability

Asma B.M. Buanz, Claudia C. Belaunde, Nina Soutari, Catherine Tuleu, Mine Orlu Gul and Simon Gaisford*

UCL School of Pharmacy, University College London, 29-39 Brunswick Square, London, WC1N 1AX, UK.

* Corresponding author

Email: s.gaisford@ucl.ac.uk

Tel: +44(0) 207 753 5863

Fax: +44(0) 207 753 5942

Abstract

The aim of this work was to compare and contrast the mechanical properties and physical stabilities of oral films prepared with either thermal ink-jet printing (TIJP) or solvent casting (SC). Clonidine hydrochloride was selected as a model drug because of its low therapeutic dose and films were prepared using cellulose polymers. Mechanical testing showed that printed films had Young's moduli and tensile strength values similar to the free film, while casted films were significantly more brittle. The drug also appeared to crystallise out of casted films during stress testing whereas printed films remained unchanged. The dissolution behaviour of printed and cast films were similar, because of the rapid disintegration of the polymer. The conclusion is that printing resulted in a better film than casting because the drug resided *on* the film, rather than *in* the film where it could exert a plasticising effect.

Key words

Thermal inkjet printing, oral films, clonidine, dynamic mechanical analysis, critical humidity.

1. Introduction

Oro-dispersible films (ODFs) have gained a lot of attention in recent years as a novel technology to overcome some of the common issues associated with conventional oral dosage forms, such as difficulty of swallowing (tablets and capsules) and stability (solutions and suspensions) (Banbury and MacGregor, 2011; Jeong et al., 2010; Saigal et al., 2008). ODFs are the size of a postage stamp and typically made from good film-forming polymers that dissolve or disintegrate rapidly upon contact with saliva (Banbury and MacGregor, 2011). They are flexible, which makes transportation and consumer handling much easier (Borsadia et al., 2003), and their manufacture can be cost effective (Reiner et al., 2010).

ODFs are not, however, without drawbacks. One is their limited drug loading capacity, which makes them most suitable for highly potent, low-dose active pharmaceutical ingredients (APIs). Other limitations include the need for solvents and heat in the manufacturing process and the issue of taste masking. The main formulation challenge is to produce films with a rapid disintegration/dissolution time without compromising mechanical properties (Hoffmann et al., 2011).

Well-established technologies such as solvent casting (SC) and hot-melt extrusion (HME) are used commercially to manufacture ODFs. In either case a polymer network is produced that is cut into strips of the required size. Both methods require the drug and the polymer to be mixed prior to forming the film. HME processing may not be suitable for APIs that are thermally labile or are degraded following shear stress (Janßen et al, 2013). One issue is that ODFs manufactured via these methods are essentially solid amorphous dispersions, with the API molecularly dispersed in the polymer matrix. It is well known that small molecular weight organic compounds typically exert a plasticising effect on polymers, which means the mechanical properties of the film may change depending on the amount and/or chemical

structure of the API incorporated. A further concern is that if the drug is formulated at a super-saturated concentration, relative to its solubility in the polymer, it is likely to phase separate by crystallising during storage. Crystallisation could potentially change the mechanical properties of the film, alter the dissolution rate, change the mouth feel and/or taste of the product and possibly alter the *in-vivo* fate of the drug (Cespi et al., 2011).

An alternative route of manufacture is to cast a free film and then deposit the API onto it. One approach is to use flexography (a contact printing method that uses rotating rollers to deposit the printing solution onto the substrate). Genina et al (2012) used flexographic printing to formulate films for controlled release while Janßen et al (2013) used flexography to dispense rasagiline mesylate solution and tadalafil suspension onto hydroxypropylmethylcellulose films. Incorporation of hydroxypropylcellulose seemed to reduce drug crystallisation after printing. However, the main limitations of flexography are the risk of contamination, the relatively low resolution and the need to prepare a print roller, which means it is most suited to medium-scale production runs (Gonzalez-Macia et al., 2010).

The API may also be deposited with thermal inkjet printing (TIJP). TIJP has the advantage of being able to deposit very small volumes (5-15 pL per droplet) with high precision. We have demonstrated before the deposition of low doses of salbutamol sulphate onto commercially available starch-based films with using conventional desktop printers (Buanz et al., 2011). TIJP technology has also been used to manufacture modified-release dosage forms by printing dots of solution onto a substrate (Scoutaris et al 2011, 2012) and it has been shown possible to fabricate three-dimensional particles by printing aqueous droplets into liquid nitrogen and subsequently freeze-drying (Mueannoom et al, 2012; Sharma et al, 2013).

Since TIJP deposits API solution *onto* a substrate, rather than dispersing API *within* a substrate, it seems reasonable to assume that printed films would maintain mechanical properties similar to that of the free film, and hence offer potential benefits compared with solvent casting for ensuring long-term stability. Testing this hypothesis is the specific aim of this work. Clonidine (CLN) was selected as a model drug. Clonidine is an antihypertensive drug that acts centrally by blocking α2-adrenoreceptors. It also has sedative and analgesic effects (Ambrose et al., 2000). The drug is available as tablets of 100 and 300 µg as the chloride salt (Paediatric Formulary Committee, 2011) and the required dose to induce pre-operative sedation is 1- 5 µg/kg (Bergendahl et al., 2006). Such low doses make CLN an ideal candidate for formulation as oral films.

2. Materials and methods

2.1 Materials

CLN, polyvinyl alcohol (PVA) 98% hydrolysed (Mw 13000-23000) and carboxymethylcellulose sodium salt medium viscosity (SCMC) were purchased from Sigma Aldrich (UK). Glycerol (analytical grade) was purchased from Fischer Scientific (UK). Bidistilled water (99.5%) was purchased from VWR International Ltd (UK), and methanol, absolute ethanol and acetonitrile (HPLC grade) were all purchased from Fischer Scientific (UK). Sodium 1-hexanesulphate (99%) was purchased from Acros organics (USA).

2.2 Film preparation

Films were prepared either by solvent casting or ink-jet printing. Concentrations were based on the minimum and maximum doses for sedation for children aged 6 months, 5 and 14 years (Table 1).

2.2.1 Printed films

The free film was composed of PVA and SCMC at 1:1 ratio with 24%w/v glycerol (Soutari et al, 2012). PVA (3.75g) was first dissolved in water (about 100mL) by heating to 80°C with continuous stirring. SCMC (3.75g) was then added and the solution was left to cool to room temperature with mixing, following which glycerol was added (36g) and the final volume was adjusted to150mL with water. The solution was poured into a non-stick baking tray (450cm^2) and dried in an oven at 30°C. The resulting film sheets were used as substrates for printing.

An HP printer (HP Deskjet 460, Hewlett-Packard Inc.) was used to print drug solution onto the film. Solutions of CLN (50mg/mL, prepared in 20% v/v methanol in water with 10%v/v glycerol) were printed from an HP 338 black cartridge. The cartridge was prepared by cutting off the top, removing the ink and rinsing with absolute ethanol. A 2cm x 2cm black template was created in Word 2007 (Microsoft Inc., USA) and used to fire the cartridge. It was found that per print pass, 316.0 µg of CLN were deposited per strip (4cm^2), equivalent to 79.0 µg/cm^2. This value was then used to prepare CLN solutions suitable for printing films with doses equivalent to those given in Table 1.

2.2.2 Casted films

Appropriate volumes of CLN solutions (3.3, 1.18, 0.66, 0.5, 0.24 and 0.1 mg/mL to prepare 250, 90, 50, 38, 18 and 7.6 µg/strip, respectively) were added to a PVA:SCMC solution (prepared as above) to obtain the required dose. Solutions were left to stir for one hour and then were cast in a non-stick baking tray and dried at 30°C. The resulting films were cut to the required size (4 cm^2) and stored over silica gel in a desiccator until use.

147 2.3 Drug content analysis

148 Films were dissolved in a solution of 20% methanol in water (4 cm² in 20 mL).
149 Solutions were filtered through a 0.45 µm filter (Millex syringe-driven filter unit,
150 Millipor Ltd, Ireland). The filtrate was analysed with high performance liquid
151 chromatography (HPLC) equipped with a UV-diode-array detector (Agilent
152 Technologies 1200 series, Germany). The mobile phase was a mixture of 0.1% v/v
153 triflouroacetic acid in water and acetonitrile (80:20% v/v) delivered at a rate of 1.0
154 mL/min. The stationary phase was a Phenomenex Synergy max C-12 column
155 (250mm x 4.6mm x 4µm; Phenomenex Synergy max, USA) kept at 40°C and the
156 injected sample volume was 10µL. Peaks were evaluated at 220nm. The percentage
157 recovery calculated for solutions made with blank film sheets dissolved in the
158 solutions spiked with known amount of CLN (in the range of 100 to 300 µg/mL, n=9)
159 was 98.29 ± 1.82%. Limit of detection and limit of quantification were found to be
160 0.15µg/mL and 0.68µg/mL, respectively. Method calibration was performed with a
161 series of standard CLN solutions in 20% methanol in water. A linear response was
162 seen between 0.25 and 100 µg/mL (r^2 =0.9997).

163

164 2.4 Characterisation of films

165 2.4.1 X-Ray Powder Diffraction (XRPD)

166 Powder diffraction data were collected with a PW3830 diffractometer (Philips,
167 Netherlands) operated with Cu K-alpha radiation (λ = 1.540598 Å) at 45 kV and 30
168 mA. Scanning was performed from 5° to 30° 2θ at 0.02° step size and 2.85 seconds
169 per step. Xpert data viewer software (PANalytical B.V, Netherland) was used to
170 analyse the data.

171

172 2.4.2 Thermogravimetric analysis (TGA)

173 Measurements were performed with a Pyris-6 TGA (PerkinElmer, UK). Samples were
174 heated at 10°C/min using nitrogen as purge gas (20mL/min). Data collection and

175 analysis were performed using Pyris software (version 3.18). Mass loss (%w/w)
176 and/or onset temperature were calculated and reported as mean ± SD.
177
178 2.4.3 Fourier Transform Infrared (FTIR)
179 FTIR spectra were collected with a PerkinElmer Spectrum 100 FTIR spectrometer in
180 the range of 4000 to 650 cm^{-1} at ambient conditions. Spectra were analysed with
181 Spectrum Express software (application version 1.02.00.0014, 2008).
182
183 2.4.4 Tensile testing
184 An Instron Universal Testing Instrument (Model 5567, Instron Ltd, Norwood, USA)
185 was used to measure the mechanical properties of films (2cm x 2cm) at a rate of
186 10mm/min and 100N static load (2kg). The cut-off point was when the film was
187 completely separated into two pieces. The tensile strength and Young's modulus
188 were measured. Data were analysed using Bluehill software 2 (version 2.6).
189
190 2.4.5 Dynamic Mechanical Analysis (DMA)
191 A Q800 Dynamic Mechanical Analyser (TA instruments, Waters LLC) was used to
192 measure the mechanical properties of the films. Advantage software for Q series
193 version 2.8.0.394 was used to collect the data and TA Universal Analysis software
194 (V4. 7A TA 2000) to analyse the data. Samples were held in a film tension clamp.
195 Experimental parameters were amplitude, 15-20um; preforce load, 0.01N; force
196 track, 125%; frequency, 10Hz. Experiments were performed at 3°C/min from room
197 temperature to 200°C.
198
199 2.4.6 Polarised light microscopy (PLM)
200 A Nikon microphot-FXA light microscope was used to collect optical images with an
201 Infinity 2 digital camera and capture application software (version 3.7.5).
202

2.4.7 Dynamic Vapour Sorption (DVS)

Films were placed in a glass pan for Dynamic Vapour Sorption (DVS-1) (Surface Measurement Systems, London, UK) at 30°C and kept at 0% RH for 90 minutes. Relative humidity was then scanned from 0 to 95% with intervals of 5% RH over 10 minutes. The change of sample weight due to water uptake or loss was recorded gravimetrically with the ultra-microbalance. The relative humidity (RH) around the sample was controlled by mixing saturated and dry carrier gases (Nitrogen) with electronic mass flow controllers.

2.4.8 Thickness and disintegration

Thickness of films (2cm x 2cm) was measured using a digital micrometer at five points of each sample, at the four corners and the centre in triplicate, and reported as mean ± SD.

The disintegration test described by Zhao et al (2009) for capsule and tablet coatings was modified to suit oral films. A device was constructed to hold the film between two clamps and a weight of 725mg was placed on top of the film. The disintegration medium used was 15 mL (37 ± 1 °C) of a simulated saliva solution (Peh and Wong, 1999) containing Na_2HPO_4 (2.38 g), KH_2PO_4 (0.19 g) and NaCl (8 g) in distilled water (1 L). The pH of the solution was adjusted to 6.75 with phosphoric acid. The time taken for the film to break was measured by filming with a black and white CCD camera (model ART-CAM-130MI-VM). Images were analysed with FTA 32 software (Version 2.0, First Ten Angstroms Inc, USA). The disintegration time was calculated as the time between adding the disintegration medium and visual observation of the film breaking (n = 3).

229 2.4.9 *In vitro* drug release

230 Dissolution tests were conducted in a water-jacketed glass vessel (outer and inner
231 diameters of 8 and 6 cm, respectively and 150mL capacity). Films were placed on a
232 plastic sieve of 3cm in diameter and 40 mL of simulated saliva solution was used as
233 a dissolution medium. A PTFE magnetic stirrer was used for agitation (size of 10cm x
234 6cm) and the temperature was maintained at 37 ± 1 °C with the help of a
235 refrigerating/heating circulator with programmable digital temperature controller
236 (Polyscience, Division of Preston Industries, Inc., USA). Samples of 1mL were
237 collected at time intervals of 0.5, 1, 2, 4, 8, 12, 16 and 30 min and replaced with a
238 fresh medium kept at ~ 37 °C. Samples were then filtered through 0.45 μm filters and
239 analysed with HPLC in accordance with the method above.

240

241 2.5 Statistical analysis

242 Results were analysed and compared with Student t-test (α=0.05) using Origin® 8.6
243 software (OriginLab Corporation, USA).

244

245 **3. Results and discussion**

246

247 3.1 Drug content and dose uniformity

248 The amount of CLN deposited by printing showed a linear correlation with the drug
249 feed solution concentration as shown in Figure 1 (r^2 = 0.9997). This is consistent with
250 the salbutamol sulphate (SS) data reported in an earlier study (Buanz et al, 2011).
251 Films prepared by blending CLN with the polymer and casting had a lower drug
252 content than films prepared by printing (Table 2). The variation of dose was higher
253 with solvent casting method (CV= 10.8 ± 6.0%) compared with printing (CV= 2.5 ±
254 2.2%). The higher dose variability in casted films may be a result of inhomogeneity in
255 blending or variability in film thickness, but the results immediately indicate the

potential utility of ink-jet printing for preparing low dose and narrow therapeutic index medicines.

3.2 Characterisation of films

In general, pharmaceutical polymer films should have good flexibility, elasticity and softness but possess enough strength to withstand mechanical stresses during manufacturing and dispensing (Preis et al., 2013; Prodduturi et al., 2004). Hydrophilic polymers are commonly used in pharmaceutical oral dosage forms (Prodduturi et al., 2004), which generally means that exposure to humidity during storage and use can affect their properties (Gontard and Ring, 1996). Here, mechanical testing and polarised-light microscopy were used to characterise the films after manufacture and following exposure to elevated humidity.

3.2.1 Tensile test

Tensile stress at the break point and Young's modulus were calculated for drug-loaded films (Table 3). Films prepared by SC had higher tensile stress values, which indicates that the films were harder than those made by TIJP (Garsuch and Breitkreutz, 2010). Skulason et al (2009) reported that Carpabol films prepared by SC have high tensile strength and low elasticity. In general, higher Young's modulus values for films made by SC also reflect their increased brittleness (Biliaderis et al., 1999).

Residual water in films can affect their mechanical properties and lead to increased elasticity by its plasticizing effect (Karisson and Singh, 1998) and thus any variation in water content between films prepared by TIJP and SC could be the reason for the difference in their mechanical properties. However, as shown by values of water content given in Table 3, the difference was not significant ($p > 0.05$). This suggests that location of drug within the films is in fact the critical factor.

3.2.2 Glass transition measurement

XRPD patterns shown in Figure 2 confirm the amorphous nature of the free and drug-loaded films. The glass transition temperature (Tg) of a polymer is one of the important parameters that reflects its mechanical properties with temperature and is associated with a small change in the heat capacity of the system due to the strong glass forming properties of polymers (Fadda et al., 2010). There is no single temperature at which Tg occurs; rather, the value depends on the technique and experimental parameters used to measure it.

DMA was used to measure the glass transition temperatures of the films. Tg is usually defined as a peak in the tan delta signal (the ratio of the storage to loss moduli) or the inflection point of the decrease in storage modulus (Gontard and Ring, 1996). Here, it was not possible to use either point. The storage modulus data are shown in Figure 3. It is apparent that there is an increase in storage modulus after 100 ^{o}C. This is because the films lost water during heating and so became very brittle. Similarly, there was no peak in the tan delta signal (data not shown) because the polymers thermally degraded. This highlights one significant problem when using thermal methods at slow heating rates. The increase in temperature acts to dry the sample and since water is often a plasticiser the mechanical properties of the film change during measurement. Hence, it was not possible to determine the Tg values of the films.

FTIR data, however, did show evidence of CLN-polymer interactions at room temperature (Table 4). Shifts are noticeable in the bands at 3274.8 (broad), 2941.6 and 1380.5 (from the free film) in the drug-loaded films, which can be assigned to hydroxyl (OH) stretch, and carbon-hydrogen (C-H) stretch and C-H bend, respectively (Coates, 2000), suggesting that the drug interacts with PVA but not with

312 SCMC, possibly through hydrogen bond with the PVA OH group. Larger shifts from
313 the free film values are seen in the case of SC samples, indicating the drug is more
314 dispersed in the polymer matrix than in the printed films. It is noticeable that the main
315 bands characteristic for CLN, such as the secondary amine N-H stretch, bend and
316 aliphatic secondary amine C-N stretch (at 3330, 1649 and 1338) are not seen, which
317 could be because they are masked by peaks from the polymers or because the drug
318 concentration is very low.
319
320 3.2.3 Critical humidity measurement
321 The critical humidity (cRH) is the humidity at a particular temperature that will cause
322 a phase transition (such as glass transition). Its determination is important along with
323 the threshold temperature in order to define the storage conditions required to
324 prevent phase changes during processing and storage (Burnett et al., 2004).
325
326 DVS is commonly used to determine cRH. cRH is usually taken to be the RH where a
327 reduction in mass is seen, corresponding to expulsion of absorbed water as the
328 sample crystallises. For CLN films the sample weight continued to increase with a
329 increasing of RH (Figure 4), and so it was not possible to determine a cRH value.
330 Presumably, this is because the majority of the sample is polymer. The method of
331 preparation (TIJP or SC) did not seem to have an effect on water sorption at lower
332 humidity as the changes of weight with time (and humidity) of both samples appear to
333 be superimposed. However, at higher humidity a higher weight increase is observed
334 for printed films. Possible reasons for this difference are discussed below.
335
336 3.2.4 Physical stability
337 Stability here refers to physical form rather than chemical degradation. Upon
338 exposure to increased temperature and/or humidity the films may absorb water and

339 be plasticised thus increasing the rate of molecular mobility of dispersed drug
340 molecules and potentially causing phase separation by crystallisation.
341
342 Films containing the highest doses of CLN (90 and 250 µg/strip) were subjected to
343 high temperature and humidity (60°C and 75 %RH) in the DMA for about 13 hours.
344 The DMA signal (storage modulus) did not change after initial equilibration to the test
345 parameters. This indicates that there was no significant change in the mechanical
346 properties of the films over the test period. However, PLM images (Figure 5) showed
347 clear signs of crystallisation in the 250 µg/strip prepared by SC. No such
348 crystallisation was observed for the lower dose film prepared by SC or films prepared
349 by TIJP.
350
351 In addition, the films used during the DVS and DMA experiments were also checked
352 with PLM (Figure 6). These films were exposed to relative humidity from 0 to 90% RH
353 at 30°C. No signs of crystallisation can be seen in films tested with DMA but clear
354 crystallisation is evident in the 250 µg/strip films prepared by SC tested with DVS and
355 the beginning of crystal growth is seen in the 90 µg/strip films. Drug in films prepared
356 by TIJP showed no evidence of crystallisation.
357
358 3.2.1 Disintegration and drug release
359 Typical disintegration times for ODFs range from 5 to 30 s (Banhart, 2008). There
360 have been several attempts to mimic *in vivo* conditions, particularly the low volume of
361 saliva, such as the slide frame method and the Petri dish method (Garsuch and
362 Breitkreutz, 2010; Hoffmann et al., 2011). Measurement of the contact angle with
363 time as a drop of water is placed on a film has also been used to assess
364 disintegration (Garsuch and Breitkreutz, 2009). The lack of official tests makes the
365 comparison between various published results a challenging task.
366

Here, the images for film disintegration were captured with the help of a CCD camera, allowing precise time measurement. For the dissolution test a volume of 40 mL was the lowest that allowed the film (placed on the plastic mesh) to float freely while the medium was mixed. The results of both tests are described below.

The results from the disintegration test show that the time taken for the samples to disintegrate is in the range of 20 to 60 s (the time recommended by the FDA is 30 s, Centre for Drug Evaluation and Research, 2008). This means that some samples exceeded the recommended limit. The main factor for that would be the thickness as it is a key factor in determining the disintegration time (Garsuch and Breitkreutz, 2010).

Figure 7 shows the release profiles of films containing 250 µg/strip of CLN prepared by either TIJP or casting (SC) in simulated saliva fluid. It is noticeable that both samples achieved more than 50 ($t_{50\%}$) and 80% ($t_{80\%}$) of drug release within 8 and 30 min, respectively. To compare the release profiles of films prepared by TIJP with films prepared by SC, difference (f_1) and similarity (f_2) factors were calculated from equations 1 and 2 (n = 3). f_2 can have a value of 0 to 100 where 100 means the profile of the tested product is the same as that of the reference and 0 means they are completely different (Costa and Sousa Lobo, 2001). The FDA adopted both factors as a way to assess the similarity of *in vitro* dissolution profiles where a value of 0 to 15 for (f_1) and 50 to 100 for (f_2) indicate the two profiles to be similar (Center for Drug Evaluation and Research, 1997). f_1 and f_2 for films containing 250 µg/strip prepared by TIJP were calculated to be 1.25 and 64.7, respectively, which means that the release profile of TIJP films is similar to that of films prepared by SC.

$$\boldsymbol{f_1} = \{[\textstyle\sum_{t=1}^{n}(\boldsymbol{R_t} - \boldsymbol{T_t})] \;/\; [\textstyle\sum_{t=1}^{n}\boldsymbol{R_t}]\} \times \mathbf{100} \qquad \textbf{Equation 3.1}$$

$$f_2 = 50\ log\left\{\left[1 + \frac{1}{n}\sum_{t=1}^{n}(R_t - T_t)^2\right]^{-0.5}\right\} \times 100 \qquad \textbf{Equation 3.2}$$

Where *n* is the number of data points and *R* and *T* are the cumulative release percentages for the reference (SC) and the test (TIJP) films at time *t*.

The release kinetics of CLN from the films were examined with four mathematical release models; zero-order, first-order, Higuchi and Hixson-Crowell models (Equations 3 to 6) (Costa and Sousa Lobo, 2001). Where Q_t and Q_0 are the amount released after time *t* and initial amount of the drug, respectively while *k* is the release constant.

$$Q_t = Q_0 + Kt \qquad \textbf{Equation 3}$$

$$\ln Q_t = \ln Q_0 + Kt \qquad \textbf{Equation 4}$$

$$Q_t = K\sqrt{t} \qquad \textbf{Equation 5}$$

$$Q_t^{1/3} = Q_0^{1/3} + Kt \qquad \textbf{Equation 6}$$

The correlation coefficients (r^2) for films prepared by TIJP or SC are given in (Table 5). The highest r^2 value was for Hixson-Crowell model. This suggests that drug release from both samples followed this model, which indicates drug release by erosion (Costa et al., 2003). This could be a result of incorporating SCMC in the formulation (Dabbagh et al., 1999; Hussain et al., 1994). This could be related to the presence of ionisable carboxylic acid group in SCMC, which increases the dissolution of the polymer (Hussain et al., 1994). Dabbagh et al (1999) noticed a decrease in matric erosion when propranolol hydrochloride was added, which they suggested to be a result of an interaction between the drug and the polymer. In this work the FTIR data presented earlier suggest that clonidine hydrochloride interacts with PVA and not SCMC in the tested films. This supports the suggestion that the carboxylic acid groups of SCMC are available for ionisation and thus allows the polymer erosion.

Hussain et al (1994) also reported that when comparing the erosion rate of SCMC matrices containing either a drug that interacts with the polymer or not, a faster rate is observed when no interaction is present.

4. Conclusion

The results indicate that films prepared by printing are significantly different in terms of mechanical properties and stability compared with films prepared by casting. In particular, the properties of the printed films are much more similar to those of the free film. It seems likely that the process of solvent casting results in a molecular dispersion of CLN throughout the polymer, analogous to a solid-amorphous dispersion. FTIR data confirm chemical interaction between the drug and the polymer. The drug appears to exert an anti-plasticising effect, increasing the brittleness of the film. When stored at elevated temperature and humidity the drug is seen to phase separate, resulting in crystal formation.

The exact nature of the printed film is harder to elucidate from the data. It is clear that immediately after printing the drug will be present in solution as droplets on the surface of the polymer film. Previous experience with printing drug solutions (Buanz et al, 2013) has shown us that the small droplets evaporate very quickly, resulting in formation of small (<5 μm) crystals. Thus, a reasonable hypothesis would be that in the printed films the drug exists either on the surface or in the top layer of the film as small crystallites. The drug is thus not acting as an anti-plasticiser and so the mechanical properties of the printed film remain similar to those of the free film. The printed film appears amorphous by XRPD because the drug content is low and small crystals do not diffract sufficiently to appear in the pattern. Upon storage at elevated temperature and humidity the printed film remains stable because it has already phase separated. Again, it is likely that the small size of any crystallites mean they were not visible with PLM.

Janßen et al (2013) did not observe any effect on the mechanical properties of films upon printing drug solutions using flexographic printing. They argue that in manufacturing oral films by this method the properties of the plain films can be assessed and it would not be necessary to evaluate the medicated films, which they envisage to add flexibility to the manufacturing process. Our work indicates a similar conclusion can be drawn in regard to ink-jet printing.

5. References

Ambrose, C., Sale, S., Howells, R., Bevan, C., Jenkins, I., Weir, P., Murphy, P. and Wolf, A., 2000. Intravenous clonidine infusion in critically ill children: Dose-dependent sedative effects and cardiovascular stability. Br. J. Anaesth. 84, 794-796.

Banbury, S., MacGregor, K., 2011. Fast-dispersing dosage forms for the pediatric market. Drug Delivery Tech. 11, 32-35.

Banhart, S.D., 2008. Thin film oral dosage forms. *Modified-release drug delivery technology*. In, Rathbone, M., Hadgraft, J. and Roberts, M., Informa Healthcare. Volume 1**:** 209-216. ISBN: 1-4200-4435-4.

Bergendahl, H., Lönnqvist, P.A., Eksborg, S., 2006. Clonidine in paediatric anaesthesia: Review of the literature and comparison with benzodiazepines for premedication. Acta Anaesth. Scand. 50, 135-143.

Biliaderis, C.G., Lazaridou, A., Arvanitoyannis, I., 1999. Glass transition and physical properties of polyol-plasticised pullulan-starch blends at low moisture. Carbo. Pol. 40, 29-47.

Borsadia, S., O'Halloran, D., Osborne, J., 2003. Quick-dissolving films- a novel approach to drug delivery. Drug Dev. Del. 3, 63-66.

Buanz, A.B.M., Saunders, M.H., Basit, A.W., Gaisford, S., 2011. Preparation of personalized-dose salbutamol sulphate oral films with thermal ink-jet printing. Pharm. Res. 28, 2386-2392.

Buanz, A.B.M., Telford, R., Scowen, I.J., Gaisford, S. 2013. Rapid preparation of pharmaceutical co-crystals with thermal ink-jet printing. *CrystEngComm.* 15, 1031-1035.

Burnett, D.J., Thielmann, F., Booth, J., 2004. Determining the critical relative humidity for moisture-induced phase transitions. Int. J. Pharm. 287, 123-133.

Center for Drug Evaluation and Research (CEDR). 2008. Guidance for industry orally disintegrating tablets. U.S. Department of Health and Human Services U.S. Food and Drug Administration

Cespi, M., Bonacucina, G., Mencarelli, G., Casettari, L., Palmieri, G.F., 2011. Dynamic mechanical thermal analysis of hypromellose 2910 free films. Eur. J. Pharm. Biopharm. 79, 458-463.

Coates, J., 2000. Interpretation of infrared spectra, a practical approach. *Encyclopedia of analytical chemistry*. Meyers, R. A. Chichester, John Wiley & Sons Ltd**:** 10815-10837.

Costa, P., Sousa Lobo, J.M., 2001. Modeling and comparison of dissolution profiles. Eur. J. Pharm. Sci. 13, 123-133.

Costa, F.O., Sousa, J.J.S., Pais, A.A.C.C., Formosinho, S.J., 2003. Comparison of dissolution profiles of ibuprofen pellets. J. Cont. Rel. 89, 199-212.

Dabbagh, M.A., Ford, J.L., Rubinstein, M.H., Hogan, J.E., Rajabi-Siahboomi, A.R., 1999. Release of propranolol hydrochloride from matrix tablets containing sodium carboxymethylcellulose and hydroxypropylmethylcellulose. Pharm. Dev. Tech. 4, 313-324..

Fadda, H.M., Khanna, M., Santos, J.C., Osman, D., Gaisford, S., Basit, A.W., 2010. The use of dynamic mechanical analysis (DMA) to evaluate plasticization of acrylic polymer films under simulated gastrointestinal conditions. Eur. J. Pharm. Biopharm. 76, 493-497.

Garsuch, V., Breitkreutz, J., 2009. Novel analytical methods for the characterization of oral wafers. Eur. J. Pharm. Biopharm. 73, 195-201.

Garsuch, V., Breitkreutz, J., 2010. Comparative investigations on different polymers for the preparation of fast-dissolving oral films. J. Pharm. Pharmacol. 62, 539-545.

Genina, N., Fors, D., Vakili, H., Ihalainen, P., Pohjala, L., Ehlers, H., Kassamakov, I., Haeggström, E., Vuorela, P., Peltonen, J., Sandler, N., 2012. Tailoring controlled-release oral dosage forms by combining inkjet and flexographic printing techniques. Eur. J. Pharm. Sci. 47, 615-623.

Gontard, N., Ring, S., 1996. Edible wheat gluten film: Influence of water content on glass transition temperature. J. Agr. Food Chem. 44, 3474-3478.

514 Gonzalez-Macia, L., Morrin, A., Smyth, M.R., Killard, A.J., 2010. Advanced printing
515 and deposition methodologies for the fabrication of biosensors and biodevices.
516 Analyst 135, 845-867.
517 Hoffmann, E.M., Breitenbach, A., Breitkreutz, J., 2011. Advances in orodispersible
518 films for drug delivery. Exp. Opin. Drug Del. 8, 299-316.
519 Hussain, A.S., Johnson, R.D., Shivanand, P., Zoglio, M.A., 1994. Effects of blending
520 a nonionic and an anionic cellulose ether polymer on drug release from hydrophilic
521 matrix capsules. Drug Dev. Ind. Pharm. 20, 2645-2657.
522 Janßen, E.M., Schliephacke, R., Breitenbach, A., Breitkreutz, J., 2013. Drug-printing
523 by flexographic printing technology—a new manufacturing process for orodispersible
524 films. Int. J. Pharm. 441, 818-825.
525 Jeong, S.H., Lee, J., Woo, J.S., 2010. Fast disintegrating tablets. In, Oral controlled
526 release formulation design and drug delivery, John Wiley & Sons, Inc.**:** 155-167.
527 Karisson, A., Singh, S.K., 1998. Thermal and mechanical characterization of
528 cellulose acetate phthalate films for pharmaceutical tablet coating: Effect of humidity
529 during measurements. Drug Dev. Ind. Pharm. 24, 827-834.
530 Mueannoom, W., Srisongphan, A., Taylor, K.M.G., Hauschild, S., Gaisford, S., 2012.
531 Thermal ink-jet spray freeze-drying for preparation of excipient-free particles of
532 salbutamol sulphate for inhalation. Eur. J. Pharm. Biopharm. 80, 149-155.
533 Paediatric Formulary Committee 2011. British National Formulary for Children.
534 London, BMJ Group, Pharmaceutical Press, and RCPCH Publications.
535 Peh, K.K., Wong, C.F., 1999. Polymeric films as vehicle for buccal delivery: Swelling,
536 mechanical, and bioadhesive properties. J. Pharm. Pharm. Sci. 2, 53-61.
537 Preis, M., Woertz, C., Kleinebudde, P., Breitkreutz, J., 2013. Oromucosal film
538 preparations: Classification and characterization methods. Exp. Opin. Drug Del.
539 10(9): 1-15.
540 Prodduturi, S., Manek, R.V., Kolling, W.M., Stodghill, S.P., Repka, M.A., 2004. Water
541 vapor sorption of hot-melt extruded hydroxypropyl cellulose films: Effect on physico-

542 mechanical properties, release characteristics, and stability. J. Pharm. Sci. 93. 3047-
543 3056.
544 Reiner, V., Giarratana, N., Monti, N.C., Breitenbach, A., Klaffenbach, P., 2010.
545 Rapidfilm®: An innovative pharmaceutical form designed to improve patient
546 compliance. Int. J. Pharm. 393, 55-60.
547 Saigal, N., Baboota, S., Ahuja, A., Ali, J., 2008. Fast-dissolving intra-oral drug
548 delivery systems. Exp. Opin. Therapeu. Pat. 18, 769-781.
549 Scoutaris, N., Alexander, M.R., Gellert, P.R., Roberts, C.J., 2011. Inkjet printing as a
550 novel medicine formulation technique. J. Cont. Rel. 156, 179-185.
551 Scoutaris, N., Hook, A.L., Gellert, P.R., Roberts, C.J., Alexander, M.R., Scurr, D.J.,
552 2012. ToF-SIMS analysis of chemical heterogeneities in inkjet micro-array printed
553 drug/polymer formulations. J. Mater. Sci. Mater. Med. 23, 385-391.
554 Sharma, G., Mueannoom, W., Buanz, A.B.M., Taylor, K.M.G., Gaisford, S., 2013. In
555 vitro characterization of terbutaline sulphate particles prepared by thermal ink-jet
556 spray freeze drying. Int. J. Pharm. 447, 165-170.
557 Skulason, S., Asgeirsdottir, M.S., Magnusson, J.P., Kristmundsdottir, T., 2009.
558 Evaluation of polymeric films for buccal drug delivery. Pharmazie 64, 197-201.
559 Soutari, N., Buanz, A.B.M., Orlu Gul, M., Tuleu, C., Gaisford, S., 2012. Quantifying
560 crystallisation rates of amorphous pharmaceuticals with dynamic mechanical analysis
561 (DMA). Int. J. Pharm. 423, 335-340.
562 Zhao, J., Gaynor, S., Schmitt, B., Coppens, K., Spaulding, W., 2009. Mechanical,
563 permeation and disintegration behavior of films based on hypromellose and its
564 blends. *2009 Annual Meeting and Exposition of the American Association of*
565 *Pharmaceutical Scientists*. Los Angeles, California.
566
567

Age/Body weight	Target dose (μg/strip)	Required feed solution conc. (mg/mL)
6 months/7.6Kg	7.6	1.20
	38	2.85
5 year-old/18Kg	18	6.01
	90	7.91
14-year old/ 50Kg	50	14.23
	250	39.54

Table 1. Clonidine hydrochloride doses and the required solution concentrations used for depositing the drug by TIJP.

Target conc. (µg/strip)	Calculated Concentration (µg/strip)					
	SC (weight-based)		SC (area-based)		TIJP (area-based)	
	Mean ± SD	% Difference	Mean ± SD	% Difference	Mean ± SD	% Difference
7.6	9.9 ± 1.3	30.1 ± 17.4	10.6 ± 0.5	39.1 ± 6.5	12.2 ± 0.4	60 ± 5.0
18	26.0 ± 2.6	44.3 ± 14.3	18.6 ± 1.0	3.5 ± 5.8	19.1 ± 1.1	5.9 ± 5.9
38	31.1 ± 15.0	-18.3 ± 39.5	30.3 ± 6.5	-20.3 ± 17	36.5 ± 1.7	-4 ± 4.4
50	51.8 ± 2.3	3.6 ± 4.5	42.7 ± 4.3	-14.7 ± 8.5	45.9 ± 0.1	-8.1 ± 0.3
90	116.7 ± 43.5	29.4 ± 48.3	73.5 ± 8.4	-18.3 ± 9.3	80.4 ± 0.4	-10.7 ± 0.4
250	226.7 ± 5.8	-9.3 ± 2.3	203.9 ± 23.9	-18.4 ± 9.6	252.8 ± 2.5	1.1 ± 1

573

574 **Table 2. A comparison between drug content in films prepared by SC and TIJP**

575 **methods.**

576

Sample	Free film	250 µg/strip	
		SC	TIJP
Tensile stress (MPa)	19.3 ± 2.9	41.9 ± 1.9	25.2 ± 1.1
Young's modulus (MPa)	547.8 ± 54.2	1423.8 ± 259.1	658.2 ± 127.6
Water content (%w/w)	8.9 ± 0.1	5.8 ± 0.3	6.6 ± 1.1
Thickness (mm)	0.1 ± 0.02	0.1 ± 0.01	0.1 ± 0.01
Disintegration time (seconds)	NA	23.3 ± 5.6	30.5 ± 4.6

Table 3. Mechanical properties, water content, thickness and disintegration times for films prepared by SC or TIJP methods.

583

Sample	TIJP 250 µg/strip	SC 250 µg/strip	Free film	PVA powder	SCMC powder	CLN powder
Wavelength (cm^{-1})	3276.4	3270.8	3274.8	3278.7	3266.8	3330.8
	2938.0	2922.4	2941.6	2942.6	NA	3082.5
	2915.8	2913.6	2917.9	2907.7	2902.7	3041.7
	1594.8	1594.5	1593.6	1417.2	1589.4	2987.1
	1415.2	1414.8	1415.3	1420.0	1413.7	2950.0
	1378.7	1375.9	1380.5	1377.8	NA	2800.0
	1321.6	1321.5	1322.0	1323.7	1324.1	2741.2
	1092.3	1091.0	1092.3	1141.8	NA	1649.3
	1037.7	1036.1	1038.5	1088.3	1037.3	1606.4
	919.7	919.3	919.7	917.0	NA	1581.1
	848.2	847.3	847.1	833.4	NA	1445.5
	NA	NA	NA	NA	NA	1435.3
	NA	NA	NA	NA	NA	1494.0
	NA	NA	NA	NA	NA	1337.6

584

585 **Table 4. Main FTIR transmittance peaks of drug-free films and films containing**

586 **250 µg/strip prepared by SC or TIJP.**

587

Sample	SC			TIJP		
	r^2	**b**	**a**	**r^2**	**b**	**a**
Zero-order	0.891	2.2	26.7	0.881	2.2	26.7
1st order	0.747	0.05	3.3	0.685	0.05	3.3
Higuchi	0.988	14.4	9.6	0.983	14.0	10.0
Hixson-Crowell	0.997	29.7	6.8	0.996	29.0	6.2

588

589 **Table 5. Regression values for the dissolution profiles for 250 µg/strip CLN**

590 **films (r^2 is the correlation coefficient, a is the intercept and b is the slope).**

591

592

593

594

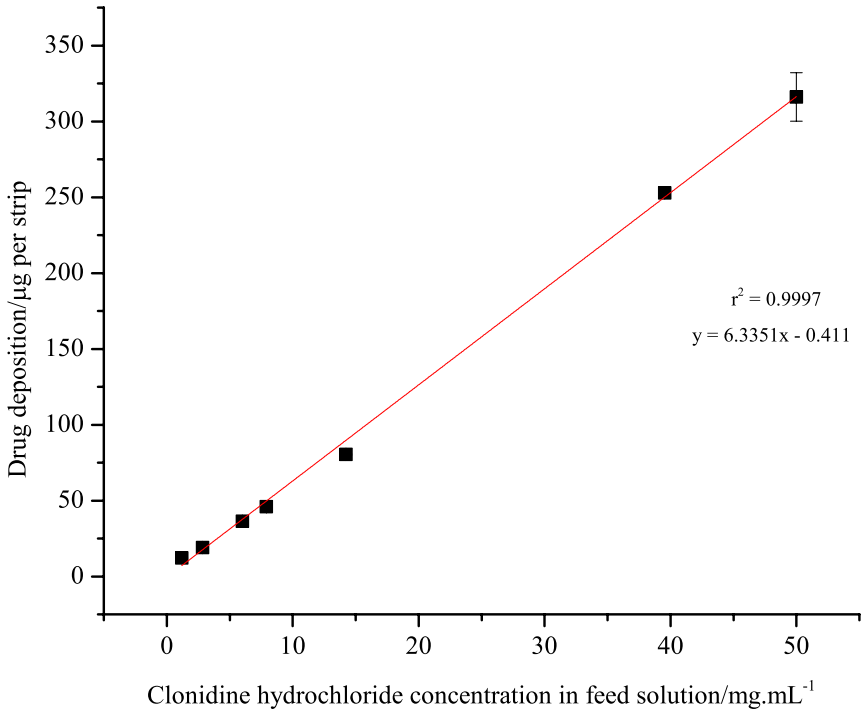

595

596 **Figure 1. Amount of clonidine hydrochloride deposited as a function of feed**

597 **solution concentration (some error bars are too small to appear on the graph)**

598

599

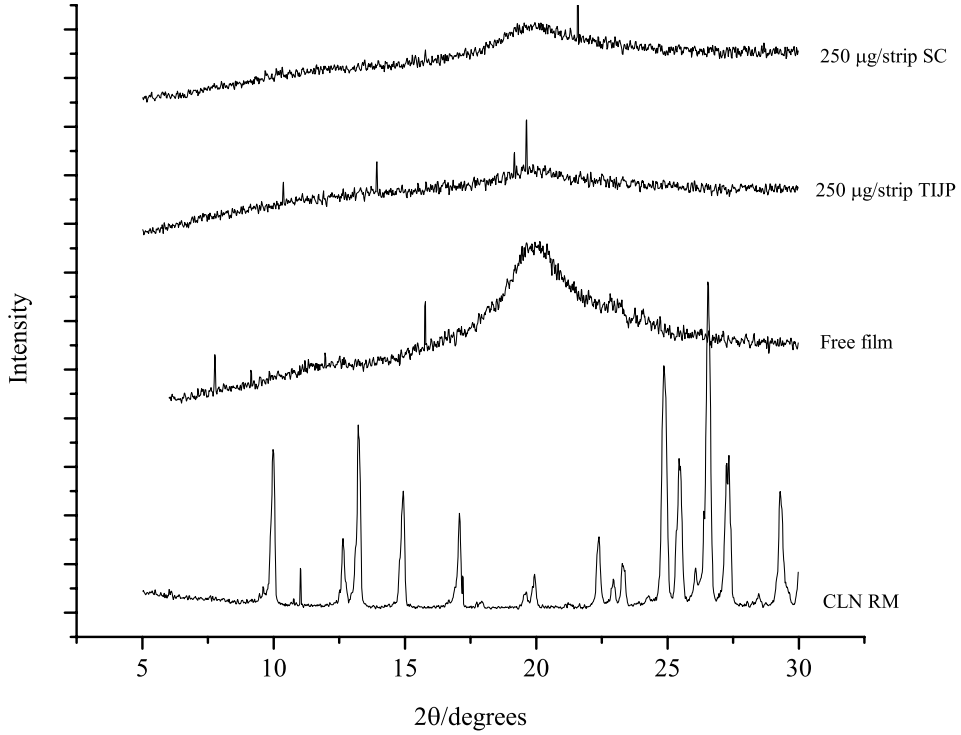

600

601 **Figure 2. XRPD patterns of medicated films prepared by SC or TIJP in**

602 **comparison to CLN raw material and the free film.**

603

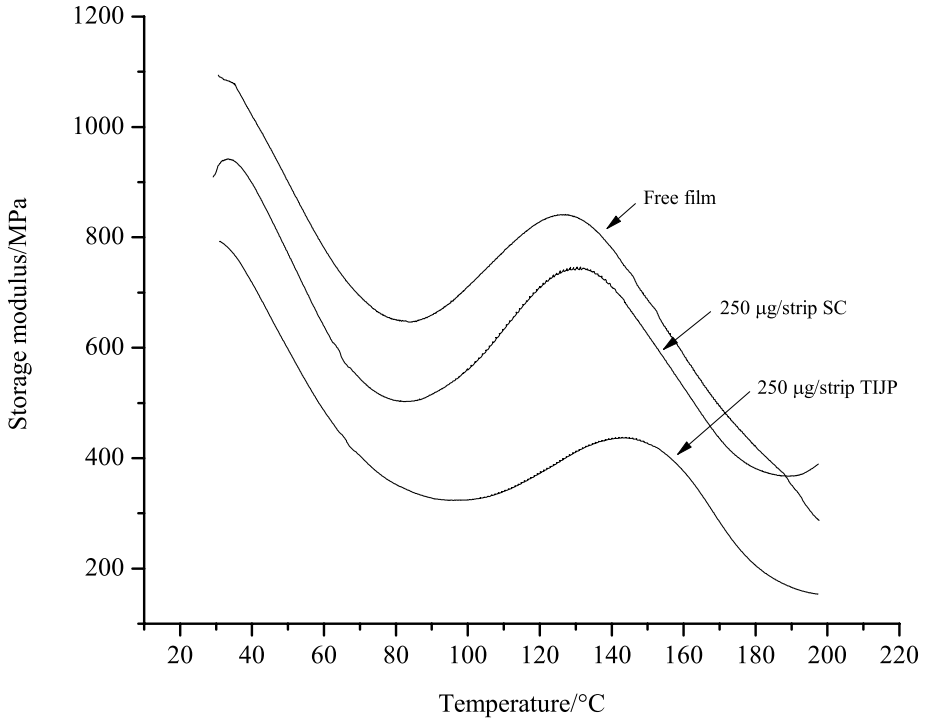

604

605 **Figure 3. Storage modulus as a function of temperature for drug-free films and**

606 **films containing 250µg/strip prepared by SC or TIJP methods.**

607

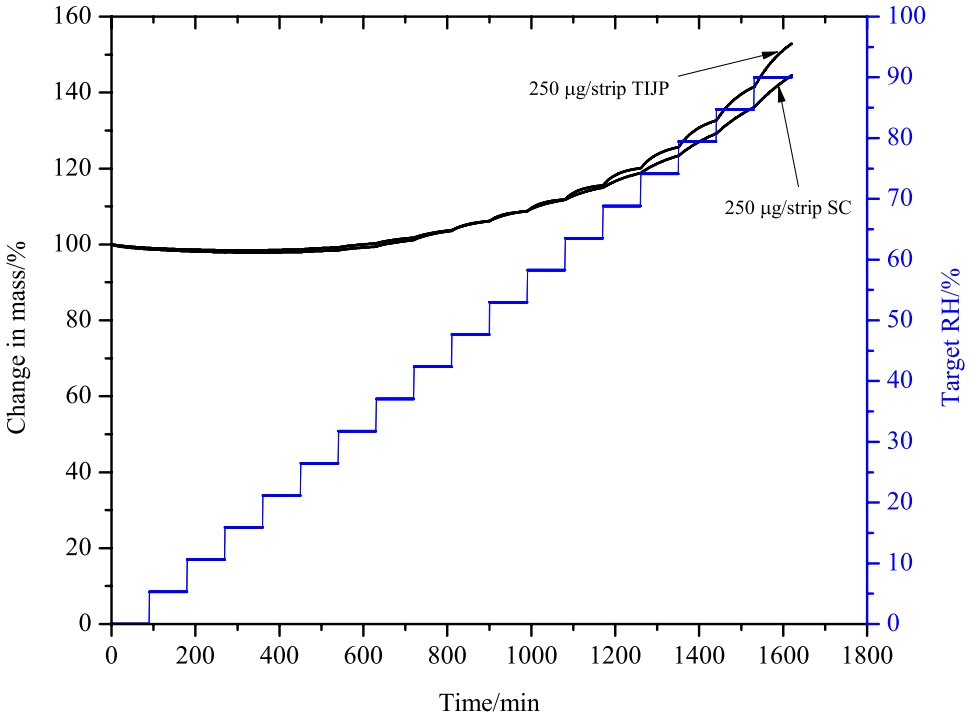

608

609 **Figure 4. DVS results of relative humidity (RH) scan for films containing 250**

610 **µg/strip prepared by SC or TIJP methods.**

611

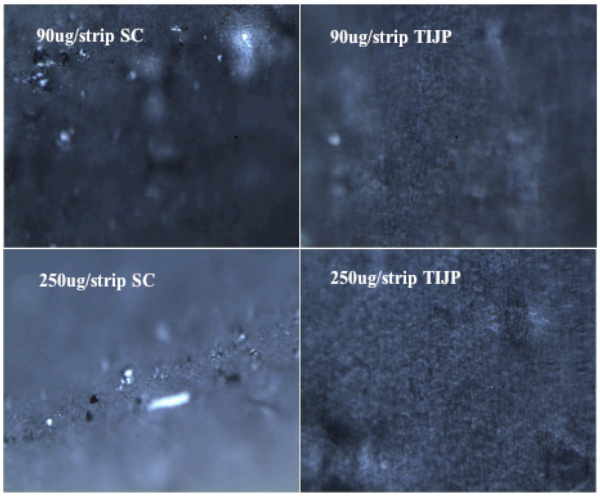

Figure 5. PLM images of films after being tested with isothermal constant humidity experiments (60°C and 75% RH) in the DMA.

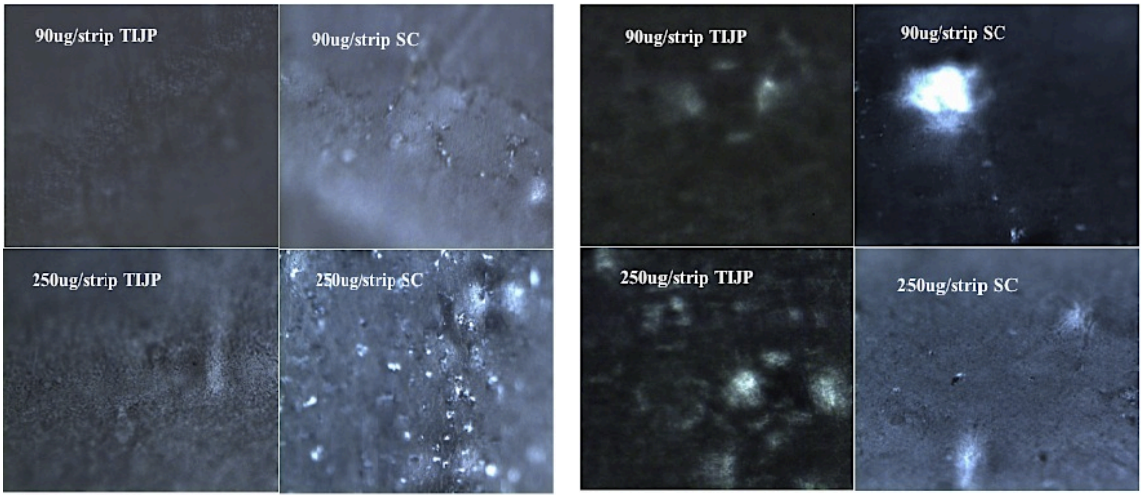

Figure 6. PLM images of films subjected to RH scan at 30°C in (left) DVS and (right) DMA.

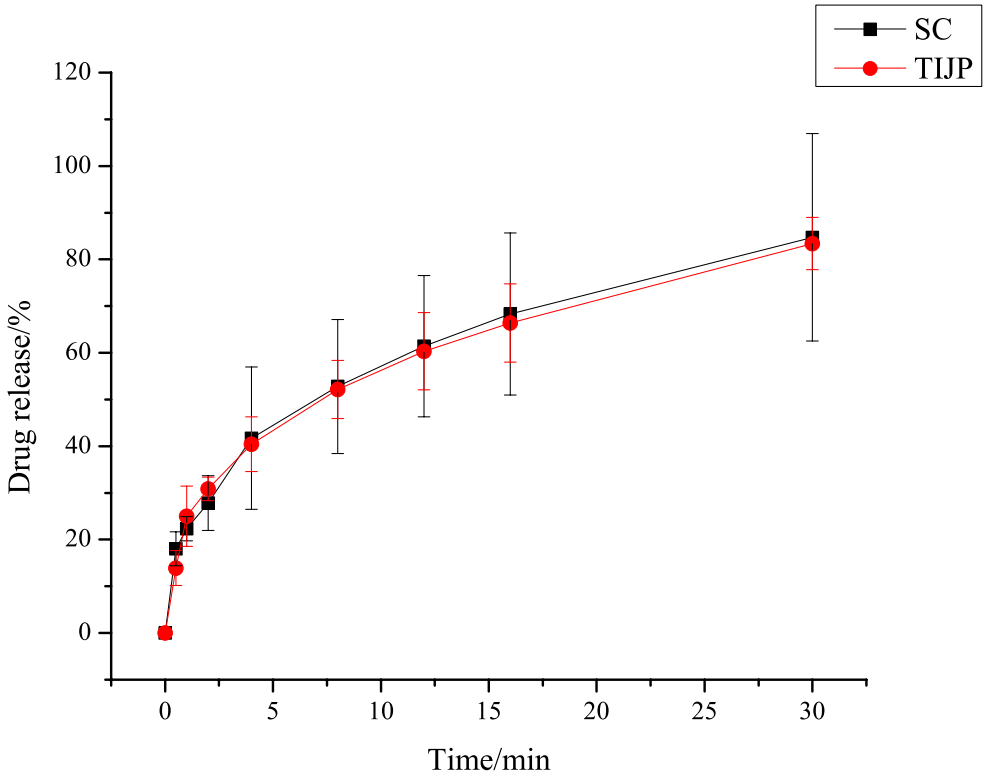

625

626 **Figure 7. Dissolution profiles for films containing 250 µg/strip CLN prepared by**

627 **SC or TIJP methods (n = 3).**

628

629